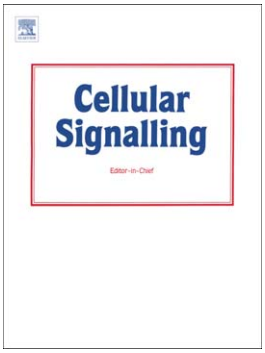

A promiscuous recognition mechanism between GPR17 and SDF-1: Molecular insights

Chiara Parravicini, Simona Daniele, Luca Palazzolo, Maria Letizia Trincavelli, Claudia Martini, Paola Zaratin, Roberto Primi, Giusy Coppolino, Elisabetta Gianazza, Maria P. Abbracchio, Ivano Eberini

PII: S0898-6568(16)30055-9
DOI: doi: 10.1016/j.cellsig.2016.03.001
Reference: CLS 8647

To appear in: *Cellular Signalling*

Received date: 10 November 2015
Revised date: 29 February 2016
Accepted date: 6 March 2016

Please cite this article as: Chiara Parravicini, Simona Daniele, Luca Palazzolo, Maria Letizia Trincavelli, Claudia Martini, Paola Zaratin, Roberto Primi, Giusy Coppolino, Elisabetta Gianazza, Maria P. Abbracchio, Ivano Eberini, A promiscuous recognition mechanism between GPR17 and SDF-1: Molecular insights, *Cellular Signalling* (2016), doi: 10.1016/j.cellsig.2016.03.001

A promiscuous recognition mechanism between GPR17 and SDF-1: molecular insights

Chiara Parravicini[a], Simona Daniele[a], Luca Palazzolo[a], Maria Letizia Trincavelli[b], Claudia Martini[b], Paola Zaratin[c], Roberto Primi[a], Giusy Coppolino[a], Elisabetta Gianazza[a], Maria P. Abbracchio[a], Ivano Eberini[a,d,]*

[a]Dipartimento di Scienze Farmacologiche e Biomolecolari, Università degli Studi di Milano, Milano, Italia,

[b]Dipartimento di Farmacia, Università degli Studi di Pisa, Pisa, Italia

[c]Fondazione Italiana Sclerosi Multipla, Genova, Italia

[d]Dipartimento di Scienze Biomediche e Cliniche "L. Sacco", Università degli Studi di Milano, Milano, Italia.

1. Chiara Parravicini: Dipartimento di Scienze Farmacologiche e Biomolecolari, Università degli Studi di Milano, Via Balzaretti 9, 20133 Milano, Italia. chiara.parravicini@unimi.it
2. Simona Daniele: Dipartimento di Scienze Farmacologiche e Biomolecolari, Università degli Studi di Milano, Via Balzaretti 9, 20133 Milano, Italia. simona.daniele@unimi.it
3. Luca Palazzolo: Dipartimento di Scienze Farmacologiche e Biomolecolari, Università degli Studi di Milano, Via Balzaretti 9, 20133 Milano, Italia. luca.palazzolo@guest.unimi.it
4. Maria Letizia Trincavelli: Dipartimento di Farmacia, Università degli Studi di Pisa, Via Bonanno Pisano 6, 56126 Pisa, Italia. ltrincavelli@farm.unipi.it
5. Claudia Martini: Dipartimento di Farmacia, Università degli Studi di Pisa, Via Bonanno Pisano 6, 56126 Pisa, Italia. claudia.martini@unipi.it
6. Paola Zaratin: Fondazione Italiana Sclerosi Multipla, Via Operai 40, 16149 Genova, Italia. paola.zaratin@aism.it
7. Roberto Primi: Dipartimento di Scienze Farmacologiche e Biomolecolari, Università degli Studi di Milano, Via Balzaretti 9, 20133 Milano, Italia. roberto.primi@guest.unimi.it
8. Giusy Coppolino: Dipartimento di Scienze Farmacologiche e Biomolecolari, Università degli Studi di Milano, Via Balzaretti 9, 20133 Milano, Italia. giusy.coppolino@unimi.it
9. Elisabetta Gianazza: Dipartimento di Scienze Farmacologiche e Biomolecolari, Università degli Studi di Milano, Via Balzaretti 9, 20133 Milano, Italia. elisabetta.gianazza@unimi.it
10. Maria P. Abbracchio: Dipartimento di Scienze Farmacologiche e Biomolecolari, Università degli Studi di Milano, Via Balzaretti 9, 20133 Milano, Italia. mariapia.abbracchio@unimi.it
11. Ivano Eberini*: Dipartimento di Scienze Farmacologiche e Biomolecolari, Università degli Studi di Milano, Via Balzaretti 9, 20133 Milano, Italia, and Dipartimento di Scienze Biomediche e

Cliniche “L. Sacco”, Università degli Studi di Milano, via Gian Battista Grassi 74, 20157 Milano, Italia. ivano.eberini@unimi.it

* Correspondig Author: Laboratorio di Biochimica e Biofisica Computazionale, Dipartimento di Scienze Farmacologiche e Biomolecolari, Università degli Studi di Milano, Via Giuseppe Balzaretti, 9, 20133 – Milano, Italia. tel.: +39 02 50318256. fax: +39 02 50318284. email: ivano.eberini@unimi.it

Abstract

Recent data and publications suggest a promiscuous behaviour for GPR17, a class-A GPCR operated by different classes of ligands, such as uracil nucleotides, cysteinyl-leukotrienes and oxysterols. This observation, together with the ability of several class-A GPCRs to form homo- and hetero-dimers, is likely to unveil new pathophysiological roles and novel emerging pharmacological properties for some of these GPCRs, including GPR17. This receptor shares structural, phylogenetic and functional properties with some chemokine receptors, CXCRs. Both GPR17 and CXCR2 are operated by oxysterols, and both GPR17 and CXCR ligands have been demonstrated to have a role in orchestrating inflammatory responses and oligodendrocyte precursor cell differentiation to myelinating cells in acute and chronic diseases of the central nervous system. Here, by combining *in silico* modelling data with *in vitro* validation in (i) a classical reference pharmacological assay for GPCR activity and (ii) a model of maturation of primary oligodendrocyte precursor cells, we demonstrate that GPR17 can be activated by SDF-1, a ligand of chemokine receptors CXCR4 and CXCR7, and investigate the underlying molecular recognition mechanism. We also demonstrate that cangrelor, a GPR17 orthosteric antagonist, can block the SDF-1-mediated activation of GPR17 in a concentration-dependent manner. The ability of GPR17 to respond to different classes of GPCR ligands suggests that this receptor modifies its function depending on the extracellular *mileu* changes occurring under specific pathophysiological conditions and advocates it as a strategic target for neurodegenerative diseases with an inflammatory/immune component.

Highlights

- GPR17 is a promiscuous class-A GPCR operated by different ligand families
- The chemokine receptor ligand SDF-1 interacts with GPR17 *via* an extended network
- SDF-1 binding to GPR17 activates intracellular heterotrimeric Gi protein pathway
- GPR17 activation by SDF-1 promotes maturation of oligodendrocyte precursor cells
- Cangrelor competitively antagonizes SDF-1 activation of GPR17

Keywords

GPR17, Class-A GPCRs, demyelinating diseases, SDF-1, chemokine receptors, neuroinflammation

Abbreviation

Stromal cell-derived Factor 1 (SDF-1)

G-protein coupled receptor (GPCR)

central nervous system (CNS)

nervous system (NS)

dorsal root ganglion (DRG)

oligodendrocyte precursor cells (OPCs)

multiple sclerosis (MS)

Protein Data Bank (PDB)

transmembrane (TM)

extracellular loops (EL)

intracellular loop (IL)

N-terminus (NT)

Steepest Descend (SD)

Conjugate Gradient (CG)

Truncated Newton (TN)

energy minimization (EM)

Generalized Born with a simple switching (GBSW)

Adopted Basis Newton-Raphson (ABNR)

root mean square deviation (RMSD)

root mean square (RMS)

room temperature (RT)

1. Introduction

Stromal cell-derived Factor 1 (SDF-1) also known as CXCL12, was isolated for the first time in 1995 from bone marrow stromal cells and identified as a chemo-attractant and proliferative factor for pre-B-cells [1]. Later studies have demonstrated additional actions for SDF-1, including important roles in immune system homeostasis, blood cells proliferation [2-4], hematopoietic stem cells homing [5, 6], foetal development, angiogenesis associated with tumour progression, carcinogenesis, HIV-1 infection and central nervous system inflammation. Nowadays, SDF-1 is recognized as one of the most influential coordinators of stem cells homing and migration [7].

SDF-1 binds two receptors, belonging to the G-protein coupled receptor (GPCR) superfamily: CXCR4 [8], the unique "non-promiscuous" chemokine receptor in the family responding to only one ligand [6], and CXCR7, whose role is still incompletely understood [9-11]. It is believed that, instead of signalling along conventional G-protein-mediated pathways, CXCR7 may act as a scavenger receptor that segregates SDF-1, reducing its extracellular availability, and thus down-regulates CXCR4 activation [11-13]. Nevertheless, recent evidence raises the hypothesis of a more specific role for CXCR7 in the modulation of SDF-1-dependent biological processes [14, 15]. In addition, several roles in the central nervous system (CNS) have been proposed for the CXCL12-CXCR4/CXCR7 axis [16, 17]. In detail, it has been demonstrated that CXCR4 contributes to the development of the nervous system (NS) [18], including the dorsal root ganglion (DRG), a source of neural stem cells that participates in endogenous stem cell-based tissue repair [7]. Moreover, survival-supporting effects mediated *via* the second CXCL12 receptor, CXCR7, have been reported for neural progenitor cells [19]. Recently, a specific contribution of SDF-1 to the differentiation of oligodendrocyte precursor cells (OPCs), the myelin producing cells in the CNS, and remyelination after traumatic and inflammatory insults, *via* the chemokine receptors CXCR4 and CXCR7, have been demonstrated *in vivo* and *in vitro* [7, 12, 15, 20, 21]. This evidence supports the hypothesis that chemokine receptors participate in the inflammatory reactions during CNS diseases *via* specific mechanisms in addition to evoking leukocyte responses. The same role in orchestrating OPC differentiation and inflammatory response in acute and chronic CNS diseases has been demonstrated for other CXCLs [7, 12, 20-22] and for ligands acting at GPR17 [23, 24], an ambiguous class-A GPCR with a spurious pharmacology. Our data showed that, in 1321N1 cells, recombinant GPR17 is activated by emergency inflammatory mediators like uracil nucleotides and cysteinyl-leukotrienes [23-25]; some research groups obtained results in agreement with ours [26, 27], whereas some others described a different GPR17 behaviour in heterologously expressing systems [28, 29]. Recent data suggest common pathophysiological roles for both CXCRs and GPR17 transduction pathways as leaders of the remyelination processes [24]. Furthermore, SDF-1 is up-regulated in

multiple sclerosis (MS) [30-32], a disease for which GPR17 has been proposed as a novel target [24, 33, 34]. Interestingly, GPR17 is only transiently expressed during the physiological differentiation of OPCs; after the immature pre-oligodendrocyte stage, it has to be down-regulated to allow cells completing maturation. Failure to do so results in inappropriate GPR17 up-regulation and OPC blockade at a pre-myelinating stage, as demonstrated in several models of CNS disease [33, 34]. Factors leading to GPR17 dysfunction in disease are currently totally unknown; their identification could help defining new strategies aimed at normalizing GPR17 function and restoring remyelination and functional recovery.

The pro-myelinating activity shared by GPR17 and CXCRs is not the only feature common to these receptors, since common promiscuous ligands have also been identified. Specifically, both CXCR2 [35] and GPR17 [36] have been recently shown to bind oxysterols, another family of ligands that are produced locally during inflammation. The latter thus represent a class of molecules acting on different class-A GPCRs with a transversal regulatory role that adds diversity to the conventional signalling pathway of each GPCR. In addition to this, CXCR2 and GPR17 do not only share the same class of 'non-conventional' endogenous modulators, but they also exhibit phylogenetically conserved structural features [37, 38]. In this respect, the hypothesis that common molecular recognition features can connect GPR17 to chemokine receptors is strengthened by the fact that GPR17 was indeed originally identified during a human genome screening for chemokine receptors [38]. The demonstration of the ability of oxysterols to cross-activate different class-A GPCRs opens the possibility that other ligands may as well operate in the same way.

The hypothesis of a triangulation among GPR17, CXCRs and some promiscuous ligands, such as SDF-1 and oxysterols, prompted us to investigate the molecular recognition mechanism between GPR17 and SDF-1. In detail, we used comparative modelling and molecular dynamics (MD) simulations to propose an updated and refined *in silico* model of GPR17 incorporating the features of all newly available suitable templates. We then predicted the interaction between GPR17 and SDF-1 by modelling the complex, and validated such predictions through reference *in vitro* experiments on both heterologously GPR17 expressing systems and on primary OPCs that natively express GPR17.

2. Material and methods

2.1 Comparative modelling of GPR17

The structure of the human $P2Y_{12}$ receptor available at the Protein Data Bank (PDB entry 4PXZ) was used as main template for modelling the transmembrane (TM) bundle of GPR17; structural information from additional templates was also taken into account, where the $P2Y_{12}$ structure was incomplete and when crystallographic artefacts had to be removed.

Most of the GPR17 structure - including TM regions, the intracellular loops (IL) 1 and 2, and all the three extracellular loops (EL) (globally residues Pro28-Leu214 and Arg235-Phe304) - was modelled on $P2Y_{12}$. Then, since in $P2Y_{12}$ the IL2 is missing, the lacking residues (Pro129-Pro135) were built using the Loop Modeler tool implemented in the MOE software (MOE 2013.10, Chemical Computing Group, Montreal, Canada). Neither $P2Y_{12}$ nor CXCR4 crystals (PDB entry 3ODU) were considered suitable for modelling IL3 because of the presence of a super-structured α-helix in TM5 connected with protein engineering to promote their crystallization. Thus, residues between TM5 and TM6 (Ile215-Val234) were based on bovine rhodopsin (Rho) structure (PDB entry 1U19), according to our alignment (see below).

In addiction, since both $P2Y_{12}$ and CXCR4 structures lack the N-terminus (NT), the first 27 residues of GPR17 (Met1-Thr27) were built using as reference template the model of CXCR4::SDF-1 published by Tamamis *et al.* [39].

In detail, the most suitable CXCR4::SDF-1 complex was selected as follows: for all the 10 MD timeframes accessible as pdb from their MD simulation, a three-step EM protocol implemented in MOE was applied. Briefly, 100 steps of Steepest Descend (SD), 100 steps of Conjugate Gradient (CG) and 10000 steps of Truncated Newton (TN) were used in sequence with a satisfactory convergence to a RMS gradient of 10^{-5} kcal/mol/Å. After EM, the complex with the lowest potential energy value was chosen as template for modelling the GPR17 N-terminus, as well as for transferring SDF-1 coordinates to the GPR17 model (complex #6, see Supplementary Materials).

Once all suitable templates had been set, comparative modelling of the GPR17::SDF-1 complex was performed using a multi template approach available in MOE (Homology Model tool). The option 'Use Selected Residues to Override Template(s)' was applied in order to override the primary template with the more appropriate ones only for the selected residues. Briefly, ten intermediate models were built as described in [36] and submitted to energy minimization (EM) to release internal constraints. The top-scoring model, according to the GB/IV scoring function, was submitted to further EM with the 'FINE' option until the RMS gradient reached a value below 0.5 kcal/mol/Å. The 'Automatic Disulfide Bond Detection' option in MOE was used to insert the conserved disulfide bridge between Cys104 and Cys181, while the disulfide bridge between Cys23 and Cys269, typical of a subgroup of related GPCRs (see below), was manually added, using the MOE Builder module.

Finally, a deeper EM protocol using the Energy Minimize tool was applied on the last GPR17::SDF-1 complex in order to reach a value of RMS gradient of 0.01 kcal/mol/Å. The CHARMM27 force field with the Reaction-field model for electrostatics was applied for the whole modelling procedure.

As already described for our previous models of GPR17 [36, 40, 41], the comparative modelling of the GPR17::SDF-1 complex was based on a global alignment performed on the primary structures of a set of GPCRs, among which GPR17, the P2Y receptor family and the known chemokine receptors. Fortynine sequences were selected containing a pair of cysteines involved in a putative disulfide bridge linking the N-terminus to EL 3. For GPR17, the short isoform (UniProt entry Q13304-2) was used.

First, the sequences were aligned using the MOE Alignment tool (which implements a version of the Needleman-Wunsch algorithm and the Blosum30 matrix) and applying GPCR constraints. In addition, the sequences of bovine Rho (UniProt entry P02699), also selected as suitable template for modelling GPR17, was realigned to the 49 sequences after fixing them with the 'freeze' option in the MOE Protein Align tool. Finally, after the CXCR4::SDF-1 complex #6 had been elected as template for modelling the first 27 residues of GPR17, the alignment of the two receptors was manually fixed using as reference a global T-Coffee alignment performed on the whole 49 sequences above. The alignment of the two query sequences was then manually modified up to Pro28 and Asn35 (in GPR17 and CXCR4, respectively), thus including the cysteines involved in the disulfide bridges as reference constraints (Cys23 and Cys28 in GPR17 and CXCR4, respectively).

2.2 Molecular dynamics simulation

The predicted GPR17::SDF-1 complex was subjected to EM followed by MD simulations by using the Generalized Born with a simple switching (GBSW) model [42] of implicit membrane/solvent implemented in the CHARMM package [43] and described in [44]

The implicit solvation model was set up employing a smoothing length of 0.6 Å; the surface tension coefficient (representing the nonpolar solvation energy) was set at 0.03 kcal/mol $Å^2$; the membrane thickness centred at Z = 0 was set at 30.0 Å with a membrane smoothing length of 5.0 Å, and the grid spacing for lookup table was set at 1.5 Å. Furthermore, before starting the MD simulations, the complex was oriented along the Z axis in membrane using the PPM server [45].

After a brief step of EM performed with the Adopted Basis Newton-Raphson (ABNR) method, the system was heated to 300 K in 500 ps with a 1.5 K increment every 2.5 ps. Velocities were randomly assigned from a Gaussian distribution. After heating, the system was allowed to equilibrate for 500 ps and then the temperature was kept constant during the 43 ns production phase applying the Berendsen weak coupling thermostat [46].

During heating, equilibration, and production phases the lengths of the bonds involving the hydrogen atoms were fixed by the SHAKE algorithm, allowing an integration time step of 2 fs; the leapfrog verlet integrator was employed to numerically integrate Newton's second law of motion and the trajectory was saved every 500 steps, allowing to write a frame per ps. All the MD simulations were performed using the all-atom CHARMM36 force field.

The trajectory was then analysed using GROMACS [47] analysis tools supported by the VMD plugins [48].

2.3 Docking simulations

The *in silico* accurate docking of cangrelor was carried out with the Dock program of the MOE Simulation module, as previously described in [36]. Briefly, the binding site of GPR17 was identified through the MOE Site Finder program. After generating a conformational database by sampling rotable bonds, cangrelor was docked onto GPR17 model using the 'Rigid Receptor' protocol, by the Triangle Matcher placement methodology. The accepted poses were scored according to the London dG scoring. The best 100 top scoring solutions were submitted to a further refinement step, based on molecular mechanics (MM). During the course of the refinement, long-range dipole-dipole interactions were calculated using the reaction field functional form for the electrostatic energy term. The final energy was evaluated using the GBVI/WSA dG scoring function with the MMFF94x forcefield.

2.4 Interaction energy decomposition

The interaction energies of the complexes GPR17::SDF-1 and GPR17::cangrelor, computed through the MMFF94x forcefield, were decomposed according to the contribution of each individual residue through an SVL script by Homan Shadnia [49], modified in our laboratory in order to remove the energetic interaction cutoffs.

2.5 [^{35}S]GTPγS binding assay

Control and 1321N1 cells stably transfected with pcDNA3.1 and HA-tag GPR17 [50] were homogenized in 5 mM Tris/HCl and 2 mM EDTA (pH 7.4) and centrifuged at 48,000 g for 15 min at 4 °C. The resulting pellets (plasma membranes) were washed in 50 mM Tris/HCl and 10 mM $MgCl_2$ (pH 7.4) and stored at -80 °C until used. Cell membranes (20 µg of proteins) were incubated with increasing SDF-1 concentrations (0.01-10 µM) and GTPγS binding to activated G proteins was quantified as previously described [51].

The specificity of SDF-1 binding to GPR17 was then evaluated. Aliquots of membranes were pre-incubated for 10 min with different concentration of a GPR17 antagonist, cangrelor (0.1-100 nM) [24, 40, 52] before addition of a fixed SDF-1 concentration (1.5 nM), corresponding to a concentration of approx. 10 fold over the EC_{50} value.

For the analysis and graphic presentation of [^{35}S]GTPγS binding data, a nonlinear multipurpose curve fitting computer program (Graph-Pad Prism) was used. All data are presented as the mean ± SEM of three different experiments.

2.6 OPC differentiation assay

Primary OPC cell cultures were isolated by orbital shaking from mixed glial cultures of postnatal day 2 Sprague-Dawley rat cortex, as previously described in [24, 33]. After purification, OPCs were seeded onto 13 mm-glass coverlisps (15,000 cells/coverslip) coated with poly-D,L-

ornithine (50 µg/mL, Sigma-Aldrich, Milan, Italy), and cultured for two days in a proliferating medium composed by Neurobasal (Life Technologies, Monza, Italy), B27 (2%, Life Technologies), L-glutamine (2 mM, EuroClone), and the human growth factors platelet-derived growth factor BB (10 ng/mL, Sigma-Aldrich) and basic fibroblast growth factor (10 ng/mL, Space Import Export, Milan, Italy). To promote differentiation, cells were switched to a Neurobasal medium growth factors-free containing triiodothyronine T3 (10 ng/mL, Sigma Aldrich).

After one day, OPCs were treated with human beta SDF-1 (1.2 nmol/l, Sigma-Aldrich) or vehicle for 48 hours and then fixed at room temperature (RT) with paraformaldehyde (4 %, Sigma-Aldrich) in PBS (0.1 M, Euroclone) containing sucrose (0.12 M, Sigma-Aldrich). Cells were pre-incubated for 30 min with the antagonists cangrelor (10 nM/l, The Medicines Company, Parsippany, NJ) or AMD3100 (1 µmol/l, Sigma-Aldrich), then treated with SDF-1.

2.6 Immunocytochemistry

To prevent unspecific staining, cells were first incubated for 20 min in Goat Serum Dilution Buffer (GSDB; 450 mM NaCl, 20 mM sodium phosphate buffer, pH 7.4, 15% goat serum, 0.3% Triton X-100). Labelling was then performed incubating cells in GSDB overnight at 4 °C with the primary rat anti-MBP (Millipore, Milan, Italy) or rabbit anti-GPR17 antibodies, and then for 1 hour at RT with the secondary goat anti-rat or anti-rabbit antibodies conjugated to Alexa Fluor 555 or 488 (Molecular Probes, Life Technologies). Nuclei were labelled with Hoechst 33258 (1:10,000, Molecular Probes, Life Technologies). Coverslips were mounted with a fluorescent mounting medium (Dako, Milan, Italy) and analysed with a fluorescence microscope.

3. Results & Discussion

3.1 *In silico* modelling of GPR17:: SDF-1 complex

Our pervious computational studies were mainly aimed at characterizing the binding features of small molecules to GPR17, including both putative endogenous ligands and new chemical entities [36, 40, 41, 53]. However, the recognition mode of GPR17 for large peptides, such as SDF-1, had not been investigated yet.

In the present study, we characterize the interactions between SDF-1 and GPR17 through an *in silico* approach, including the generation of a new comparative model of GPR17 and its further refinement through MD simulations.

Briefly, the model of the human GPR17::SDF-1 complex was built through a step-by-step procedure including: 1) the optimization of the structure of $P2Y_{12}$ receptor, chosen as main template for modelling the TM bundle of GPR17 [54]; 2) homology modelling of GPR17 based on selected multiple templates; 3) selection, among the available structures of the CXCR4::SDF-1 complex, recently published by Tamamis and Floudas [39], of the most suitable one as a

template for modelling SDF-1; 4) translation of the interaction network between CXCR4 and SDF-1 to the GPR17::SDF-1 model; 5) refinement of the obtained complex through MD simulation in an implicit membrane/water model.

A detailed description of the production phases of the GPR17::SDF-1 complex is reported in the following paragraphs.

3.2 Building a GPR17 comparative model

Several *in silico* models of the GPR17 receptor have been proposed by our group in the last years, following the expanding resolution of class-A GPCR structures [41, 53]. Despite the lack of templates with sequences highly identical to GPR17, the accuracy of our models was high enough to lead us to the identification of a first set of potent and diverse GPR17 ligands, chemically unrelated to the previously known nucleotide- or cysteinyl-leukotriene derivatives [40].

Since 2007, when rhodopsin was set as the class-A GPCR prototype, the increasing number of solved structures highlighted some common features that are crucial for their operability, but also revealed an unexpected structural diversity in their extracellular loops that account for their heterogeneity in molecular recognition mechanisms.

In 2010, the crystallization of human CXCR4 provided a significant improvement in the accuracy of our GPR17 modelling [36], because this structure enabled us to reliably describe the extracellular regions of the receptor (especially EL2 and the disulphide bridge linking the N-terminus to EL3): these features are crucial in the molecular recognition process [55, 56], but none of the previously available templates was suitable for their modelling.

More recently, the structure of the human $P2Y_{12}$ receptor has been solved [54], allowing a leap forward in our procedures. In fact, the P2Y receptor family is related to GPR17 not only from a pharmacological [52], but also from a phylogenetic and structural point of view, as both P2Y receptors and GPR17 belong to the purine receptor cluster of the δ-group in the rhodopsin family of GPCRs [37]. The presence, in the human $P2Y_{12}$ receptor, of a conserved disulphide bridge between the N-terminus and EL3 further validates our original hypothesis on GPR17, indicating that the constraint of the disulphide bridge Cys23-Cys269, imposed on the extracellular architecture of our model, is reliable.

A picture of the general extracellular topology of the new GPR17 model, in comparison with that of templates selected so far for modelling [36, 40, 41, 53] is shown in Supplementary Figure 1.

The architecture of the putative GPR17 ELs (panel A) significantly differs from that of rhodopsin (panel B), in which the access of ligands to the TM cavity is hampered by EL2. Instead, in our GPR17 model, in a similar way to CXCR4 (C) and $P2Y_{12}$ (D), EL2 stands in an open conformation, allowing the exposure of a wider surface for ligand recognition. This

increased binding surface due to the open EL2 conformation may be especially crucial for the recognition of large peptidic ligands like SDF-1.

To date, still in the absence of a high-resolution structure of GPR17, $P2Y_{12}$ and CXCR4 represent the best templates for modelling our target. Although the difference in identity between GPR17 and the two sequences of either $P2Y_{12}$ or CXCR4 is not significant (see Table 1), we modelled GPR17 entirely on the $P2Y_{12}$ structure, with the exception of the regions where $P2Y_{12}$ was incomplete, *i.e.* in the N-terminus, or where its structure was affected by the crystallization process, *i.e.* in EL3 (see below). This approach also allowed us to build a model of GPR17::SDF-1 complex exempt of any bias derived from the use of the claimed SDF-1 receptor CXCR4.

Table 1 - Pairwise Identity Matrix

Sequences	GPR17	$P2Y_{12}$	CXCR4
GPR17		21.6	20.5
$P2Y_{12}$	21.8		19.6
CXCR4	21.2	20.2	

Uniprot codes: human GPR17 - Q13304-2; human $P2Y_{12}$ - Q9H244; human CXCR4 - P61073.
The table value at row i, column j equals the number of residue matches between sequences i and j, divided by the length of sequence j.

As mentioned before, the lack of a whole $P2Y_{12}$ structure induced us to include additional templates in our modelling procedure. In detail, since $P2Y_{12}$, in a similar way to CXCR4, due to the fusion construct used for stabilizing the protein during crystallization, shows an over-extended α-helix at the intracellular side of TM5 and a discontinuous IL3 [54], IL3 was modelled using bovine rhodopsin as template. Indeed, despite advancements in the structural studies on GPCRs in the last twenty years, bovine rhodopsin still represents one of the few structures that did not require any protein engineering for a successful resolution [57]; for this reason, its crystal contains its whole structure, including an intact IL3.

3.3 Building the GPR17::SDF-1 complex

Several experimental findings [58], as well as the *in silico* predictions [59, 60] suggest that SDF-1 is firmly bound to CXCR4 at both the extracellular N-terminus and the TM bundle. However, none of the experimental structures is complete and provides a global picture of the molecular recognition between CXCR4 and SDF-1 [39]. This problem stems from the difficulty of 'capturing' the final conformation of the flexible CXCR4 N-terminus, which results in the lack of the first 24 residues in all the available X-ray structures of CXCR4. Recently, through a very comprehensive computational study, including an in-depth protein::protein docking with

conformational search combined with MD simulations, Tamamis and Floudas proposed a model for the CXCR4::SDF-1 interaction, in strong agreement with the most up-to-date experimental evidence. Considering the strong relationship between GPR17 and CXCR4, together with the lack of any structural information for the N-termini in both CXCR4 and $P2Y_{12}$ crystallographic structures, we were confident enough in using this model to integrate in our GPR17 model the residues missing at its N-terminus. For the same reason, when building the hypothetical GPR17::SDF-1 complex, we reproduced, by homology modelling, the conformation and orientation of SDF-1 bound to CXCR4, to then transfer its coordinates onto our model.

Ten time-frames, representing the CXCR4::SDF-1 complex, are available from the 20 ns MD simulations performed by Tamamis and Floudas. The choice of using their complex #6 for implementing our GPR17 model was based on energetic criteria. Briefly, after an in-depth multi-step EM protocol, complex #6 was associated with the lowest potential energy value with respect to all the frames evaluated (not shown).

The global topology of the resulting CXCR4::SDF-1 complex is reported in Figure 1.

3.4 Molecular dynamics simulations of the GPR17:: SDF-1 complex

In order to investigate the molecular behaviour of the GPR17::SDF-1 complex, we carried out a 43 ns MD simulation. The evaluation of the stability of the GPR17::SDF-1 complex during the production phase was based both on energetic and geometric parameters, as described in the following.

The general stability of the GPR17::SDF-1 complex is confirmed by the tendency of the MD simulations to reach convergence. In detail, the tendency to reach an equilibrium state is suggested by the trend of the total energy of the complex, which significantly decreases in the first phase and reaches a stable level in the second half of the MD simulation (Figure 2A), as well as by the root mean square deviation (RMSD) values, which after 20 ns reach a plateau around 2.5 Å for both GPR17 and SDF-1 (Figure 2C).

As expected, for SDF-1, the largest root mean square (RMS) fluctuations, computed for the α-carbons, concern the unfolded regions of the protein (in light grey, Figure 2D). In contrast to the above, the region between residues 28 and 38, even if belonging to a loop, shows lower mobility, which is probably due to its involvement in the formation of the complex with GPR17. In GPR17 (in black, Figure 2D), among the internal loops IL3 shows the highest mobility (RMSF up to 0.5 nm), followed by IL2 (RMSF up to 0.3 nm), while all the extracellular loops are associated with lower RMS fluctuations thanks to the stabilization induced by the interaction with SDF-1. Conversely, the RMS fluctuation values for GPR17 α-helices stay under 0.1 nm (Figure 2D) suggesting a very high stability for the TM barrel structure.

To evaluate the global stability of the complex, the interaction energy between the two proteins was computed during the whole production phase. As shown in Figure 2B, the interaction energy

between GPR17 and SDF-1 significantly decreases, with a variation of approx. 160 ± 20 kcal/mol, suggesting that the reciprocal interaction between GPR17 and SDF-1 is favoured. Moreover, the number of interactions occurring between SDF-1 and GPR17 confirms a suitable arrangement for the complex. In detail, as shown in Figure 2E, after an increase in the first half of the simulation, the number of contacts remains constant, suggesting that the complex approaches stabilization after approx. 20 ns. Among these contacts, several were identified as hydrogen bonds (Figure 2F); up to 50 of them are formed between pairs of atoms within 0.35 nm from one another.

Also the analysis of the secondary structure stability of both SDF-1 and GPR17 during the MD simulation suggests that the global topology of the proteins and their secondary structures are conserved (see Supplementary Figure 2). As expected, in SDF-1, the most flexible region is the unfolded N-terminus of the protein, which is directly involved in the interaction with GPR17 (see below).

During the MD, the stability of the GPR17::SDF-1 complex as well the global robustness of the helical bundle of the GPR17 model were also followed by analysing the formation of specific interactions between specific pairs of residues. Supplementary Figure 3 plots the distances between pairs of GPR17 residues likely involved in intramolecular polar interactions that are stable for the whole duration of the MD.

As reported in Supplementary Figure 3, the structure of GPR17 is stabilized by the presence of several residue pairs whose acceptor or donor groups remain within a distance consistent with an ionic or hydrogen bond interaction; this finding suggests that the global arrangement of the model is preserved during the MD simulation. In some cases, *e.g.* for the pairs Arg114-Asp128, Arg114-Asp128, Ser118-Asn189, Thr27-Hse117, Thr231-Ala132, new contacts are stabilized, through the formation of new ionic or hydrogen bonds.

Supplementary Table 1 reports the list all the interactions observed in the GPR17::SDF-1 complex during the whole MD simulation. Twenty-one pairs of these residues form interactions that have been observed as well in the Tamamis and Floudas model of the CXCR4::SDF-1 complex [39] (see Supplementary Table 1). In addition, among the conserved interactions, those involving the following pairs are stable throughout the MD simulation: Lys1-Tyr112; Lys1-Tyr251; Lys1-Asn279; Ser-Gln25; Asn33-Asn2; Gln48-Ala18; Gln48-Ala18; Gln48-Thr19; Gln48-Ala20; Glu21-Lys27 (see Supplementary Table 1). In order to visually render these interactions, we depicted them in a spatial map (Supplementary Figure 4) showing the regions most extensively involved in the molecular recognition between GPR17 and SDF-1.

In detail, the evolution of the distances between atoms involved in hydrogen bonds, salt bridges and cation-π interactions that are persistent between SDF-1 and GPR17 during the whole MD simulation are reported in Figure 3.

Lys1 of SDF-1, essential for the chemotactic activity towards CXCR4 [61], exhibits specific H-bond interactions with the -OH groups of Tyr112 (TM3), Tyr251 (TM6), and Tyr262 (EL3), and with polar groups of residues Asn279 (TM7) and Gln183 (EL2). While our previous studies on GPR17 reported that all these residues are likely involved in the recognition of uracil nucleotides [41, 53], in SDF-1 neither His255 nor Arg255 are directly involved in the recognition mechanism. Figure 4 provides a detailed picture of the N-terminus extremity of SDF-1 (in white) and GPR17 (in green) in the TM pocket.

Figure 5 focuses instead on the main interactions encompassing the extracellular region of GPR17, involved in H-bond networks (panel A) or salt bridges (panel B), respectively.

Globally, our *in silico* data suggest that the binding surface of SDF-1 on GPR17 is diffused and that both the N-terminus and the ELs are important for molecular recognition, as already described for many peptide ligands of GPCRs. In addition, TM segments are also involved.

As represented in Figure 6, the hydrophobic component (in green) of the molecular surface, rendered as van der Waals interactions between SDF-1 and GPR17, is relevant for the binding between the two proteins at both the TM pocket and the extracellular binding site; the same is true of the H-bonding pattern (in magenta). Conversely, the mild-polar interactions (in blue) are less significant for the establishment of the complex and involve mainly the extracellular domains.

In particular, our data suggest that the flexible N-terminus tail of SDF-1 deeply penetrates the TM bundle of GPR17, whose upper region represents the putative “purinergic binding” site of GPR17. Indeed, our previous studies suggest that all the small molecules identified so far as putative ligands for GPR17, whether they are endogenous or synthetic compounds, target the orthosteric TM binding site of the receptor. Among these molecules, also the nucleotide-derivative antagonist cangrelor binds the same binding pocket, establishing specific interactions with some residues involved in the SDF-1 recognition; this features suggest that cangrelor may hamper the entrance of SDF-1 N-terminus in the TM binding site. This ‘competition’ is shown in Figure 7, in which a representative docking pose of cangrelor is superimposed to the TM pocket of the GPR17::SDF-1 complex. Supplementary Table 2 reports the decomposed interaction energies for GPR17::SDF1 and GPR17::cangrelor. SDF-1 establishes a wide interaction network with GPR17 (31 amino acids), as described for class-A GPCR peptide ligands [62]; differently, cangrelor establishes a lower number of interactions with GPR17 (19 amino acids), specifically located in the already recognized binding site for uracil nucleotides [40, 41]. Seven amino acids of GPR17 are involved both in SDF-1 and cangrelor molecular recognition. Moreover, the most significant energy contribution in the GPR17::cangrelor complex is associated with Arg255, whose functional role was already described in a mutant receptor model through a computational approach [51, 53].

As for the CXCR4::SDF-1 complex, the opened conformation of EL2 allows this fitting, suggesting that the open state of EL2 is a requirement for the recognition of SDF-1 by GPR17. Although for GPR17, as for many other GPCRs, it has been already hypothesised that a conformational change in EL2 is essential for the recognition of extracellular nucleotides [53], this hypothesis remained unproved until the publication of new structures different from rhodopsin, in which the EL2 is in closed conformation.

Recently, a phylogenetic analysis based on the GPCRs crystallized so far examines the evolution of structural changes occurred in the GPCRs, focusing on the TM binding site and on EL2 [63]. The authors assume rhodopsin as representative of an evolutionary transition of peptide-binding receptors to receptors binding to small molecules, and postulate that, during this evolution, ELs had the initial role of mimicking peptidic ligands. However, purine, leukotriene and free fatty acid receptors seem to have undergone a separate evolution from peptide receptors, and, despite developing the capability to bind to small ligands, they have conserved the ability to bind to peptides, suggests a possible interchangeability of peptide and purine binding.

In agreement with this analysis, GPR17, which is able to bind to both small molecules [36, 52, 64] and peptide-like ligands (the present study), holds a conserved, well-folded, open, EL2.

3.5 *In vitro* assessment of SDF-1-mediated GPR17 activation

To validate our *in silico* predictions, we tested the ability of SDF-1 to bind to GPR17 in two different *in vitro* models: the [^{35}S]GTPγS binding assay, a well-established pharmacological assay suitable for studying GPCR activity [50, 52, 64], and primary cultured OPCs natively expressing GPR17 that can be instructed to differentiate to mature oligodendrocytes expressing the myelin protein MBP by exposure to GPR17 agonists [24, 33]

As shown in Figure 8, [^{35}S]GTPγS binding experiments performed on 1321N1 cells stably transfected with GPR17 demonstrate that SDF-1 is able to increase, in a concentration dependent manner, the GTPγS binding to cell membranes, with affinity constant values of 0.14±0.03 nM (panel A). In parallel, no significant binding stimulation was observed in 1321N1 wild-type control cells, demonstrating that this agonistic response is specifically mediated by the presence of GPR17 (data not shown).

This effect is completely antagonized by the well-known GPR17 orthosteric antagonist cangrelor, further confirming that SDF-1 specifically bound GPR17 and behaved as a receptor agonist (panel B). This evidence is also in agreement with our *in silico* data predicting that cangrelor would inhibit the SDF-1-mediated GPR17 activation.

In primary OPC cultures, treatment with SDF-1 increases by approximately 30% the number of MBP-positive cells compared to control conditions, thus accelerating their differentiation toward a mature phenotype, in line with literature data [7, 12, 20] (see Figure 9, panel A, B and F). As also shown in Figure 9, this increase is not observed when SDF-1 is added to cells either in

combination with the GPR17 antagonist cangrelor (panel C, H), or, as expected, with the CXCR4 antagonist plerixafor (panel D, H). In both antagonist groups, the number of MBP-positive cells is comparable to, or slightly lower than, the one measured in the vehicle-treated cells.

Globally, these results demonstrate that SDF-1, at a concentration able to activate its cognate receptor CXCR4, can also directly act as a promiscuous activator of GPR17, corroborating our hypothesis of a common pathophysiological role for GPR17 and chemokine receptors in leading the remyelination processes. We do not know at present to what extent activation of CXCR4 and GPR17 by SDF-1 individually contributes to the detected OPC maturation; however, our data demonstrating that each of the two tested antagonists can fully abolish the SDF-1 induced effect suggests that formation of CXCR4::GPR17 heterodimers may be involved.

4. Conclusions

In conclusion, the present data show that, besides activating its cognate receptors, CXCR4 and CXCR7, SDF-1 can also activate the P2Y-like GPR17 receptor with comparable potency [65]. In our *in vitro* models, the activation of GPR17 by SDF-1 efficiently promotes the maturation of OPCs, a well-known key event of the myelination pathway. This emphasizes the pathophysiological relevance of the cross-talk between these receptors in the regulation of OPC maturation and myelination, which is particularly relevant to the local neuroinflammatory milieu associated with MS.

The concentration range at which SDF-1 operates CXCR4, CXCR7 and GPR17 is comparable with the extracellular concentrations of this chemokine in inflamed tissues [30, 66, 67]. On this basis, we propose that, under constantly and chronically elevated SDF-1 concentrations, as it may occur under long-term inflammatory degenerative conditions, GPR17 function can be aberrantly amplified [34], thus preventing its down-regulation. As mentioned before, prolonged and abnormal GPR17 up-regulation under several pathological settings [34] results in impaired terminal maturation of OPCs that are thus frozen at an immature stage, thus blocking myelination [33]. In this respect, we believe that the pharmacological modulation of GPR17 through ligands able to counteract its excessive activation in inflammation could represent a novel strategy to restore its function in pathological conditions, especially those involving a supra-physiological activation of uracil nucleotide-, leukotriene-, oxysterol- and/or chemokine-activated signal transduction pathways.

We believe that our previous observations [35, 36], together with the new ones, strengthen the emerging idea of a complex cross-talk network among class-A GPCRs. This complexity does not only deal with the promiscuity of some of their ligands and with their availability in tissues, but also with the possibility for these receptors to homo- and/or hetero-dimerize with other class-A GPCRs, acquiring different biochemical and pharmacological properties. Understanding this

complexity via new emerging *in silico* and *in vitro* techniques and validating *in vivo* GPCR homo- and hetero-dimerization will help shedding light on the biological roles of these receptors and foster the development of novel therapeutic strategies aimed at restoring their physiological activity.

Figure Captions

Fig. 1. Comparative model of the CXCR4::SDF-1 complex. Regions built using $P2Y_{12}$ as template are represented as green ribbons; residues transferred from other templates are highlighted in yellow (IL3, from rhodopsin) and orange (N-terminus, from the CXCR4::SDF-1 complex #6 in [39]. SDF-1 (from the CXCR4::SDF-1 complex #6 in [39] is coloured in grey.

Fig. 2. Stability of GPR17::SDF-1 during MD simulation.

Total energy and interaction energy (light grey) are plotted *vs* time in panels (A) and (B), respectively. In both graphs two different bearing trends (grey and black) are drawn, each calculated using smooth.spline(), a function of R that fits a cubic smoothing spline to the data according to a spar parameter, which weighs data fluctuations.

Panel (C) shows the RMSD profiles *vs* time for SDF-1 (grey) and GPR17 (black), whereas panel (D) shows the RMS fluctuation, expressed in nm, computed for the α-carbons of SDF-1 (light grey, residues 1-68) and GPR17 (dark grey, residues 1-304).

Panel (E) reports as a function of time the total number of contacts between all pairs of residues, panel (F) the total number of hydrogen bonds occurring between SDF-1 and GPR17 (in black); panel (F) also shows the number of atom pairs less than 0.35 nm apart (in grey).

Fig. 3. Distances vs MD simulation time for couples of residues involved in stable interactions between SDF-1 (first residue) and GPR17 (second residue). For ionic bonds, H-bonds and cation-π interactions, a cut-off of 4.5 Å, 4.0 Å and 6.0 Å, respectively, between donor and acceptor groups was used.

Fig. 4. TM binding pocket of GPR17. Representative picture of the residue Lys1 (labelled sticks), at the extremity of SDF-1 N-terminus (white ribbons) entering the TM binding pocket of GPR17 (green ribbons). For representing the GPR17::SDF-1 complex, the most populated cluster within the MD simulation was chosen.

Fig. 5. Extracellular binding site of GPR17. Residues involved in the main polar interaction networks between SDF-1 (white ribbons) and GPR17 extracellular loops (green ribbons). For representing the GPR17::SDF-1 complex, the most populated cluster within the MD simulation was chosen.

Fig. 6. GPR17::SDF-1 van der Waals interaction surface. The molecular surfaces of SDF-1 (white ribbons) within the TM binding site of GPR17 (grey ribbons) computed as van der Waals

interaction surface is represented with green, magenta and blue lines for hydrophobic, H-bonding and mild polar interactions, respectively.

Fig. 7. Uracil nucleotide binding site of GPR17. Superposition between SDF-1 (light grey molecular surface and ribbons) and cangrelor (sticks, atom-type colour code) in the TM, orthosteric, binding site of GPR17 (grey ribbons).

Fig. 8. Pharmacological profile of SDF-1 to GPR17: GTPγS binding. (A) Membrane aliquots obtained from 1321N1 cells transfected with hGPR17 were incubated with different SDF-1 concentrations, and [^{35}S]GTPγS binding assay was performed as described in the Material and Method section. **(B)** Effect of the GPR17 receptor antagonist cangrelor on ligand-stimulated [^{35}S]GTPγS binding. Membranes from hGPR17-transfected cells were pre-incubated for 10 min with cangrelor (0.1 nM–100 nM), then stimulated with SDF-1 at the constant concentration of 1.5 nM (10 fold over the EC_{50} value). [^{35}S]GTPγS binding assay was performed as described in the Material and Method section. All data are expressed as percentage of basal [^{35}S]GTPγS binding (set to 100%) and are mean ± SEM of 3 different experiments, each one performed in duplicate.

Fig. 9. SDF-1-mediated activation of GPR17 in OPCs. Representative images of MBP expressing cells (in red) treated with vehicle (A) and SDF-1 alone (B), or in combination with the GPR17 antagonist cangrelor (C) and with the CXCR4 antagonist plerixafor (D). (E) Control cell cultures expressing GPR17 (in green) and MBP (in red). Cell nuclei are labelled with Hoechst 33258 (in blue). (F) Histograms show quantification of the percentage of MBP positive cells after 48 hours of treatment with vehicle (69.53%±7.59) and with SDF-1 alone (SDF-1-treated cells set to 100%, 100%±7.92), or in combination with cangrelor (C, 62.91%±7.17) and plerixafor (P, 65.88%± 7.57). The number of positive cells was counted in 40 optical fields under a 20X magnification. Data are the mean ± SEM of at least three independent experiments. *, $p < 0.05$; **, $p < 0.01$ compared to SDF-1 treated cells; Dunnett's Multiple Comparison Test. Scale bar: 50 μm.

Acknowledgements

CP was supported by a Fondazione Umberto Veronesi Fellowship. Research activity was sponsored by Fondazione Italiana Sclerosi Multipla (FISM) to MPA (2013/R/1), to IE and MPA (2013/S/2) and to LP (2014/B/5). Special thanks to prof. Francesca Fanelli, Università degli Studi di Modena e Reggio Emilia, for supporting us in the setup of MD simulation, and to drs. Elisabetta Bonfanti and Davide Lecca, Università degli Studi di Milano, for helpful discussion. Special thanks to Studio Bozzetto for the artwork in graphical abstract.

References

[1] Shirozu M, Nakano T, Inazawa J, Tashiro K, Tada H, Shinohara T, Honjo T, Structure and chromosomal localization of the human stromal cell-derived factor 1 (SDF1) gene, Genomics 28 (1995) 495-500.
[2] Lataillade JJ, Clay D, Bourin P, Herodin F, Dupuy C, Jasmin C, Le Bousse-Kerdiles MC, Stromal cell-derived factor 1 regulates primitive hematopoiesis by suppressing apoptosis and by promoting G(0)/G(1) transition in CD34(+) cells: evidence for an autocrine/paracrine mechanism, Blood 99 (2002) 1117-1129.
[3] Zou YR, Kottmann AH, Kuroda M, Taniuchi I, Littman DR, Function of the chemokine receptor CXCR4 in haematopoiesis and in cerebellar development, Nature 393 (1998) 595-599.
[4] Ma Q, Jones D, Borghesani PR, Segal RA, Nagasawa T, Kishimoto T, Bronson RT, Springer TA, Impaired B-lymphopoiesis, myelopoiesis, and derailed cerebellar neuron migration in CXCR4- and SDF-1-deficient mice, Proceedings of the National Academy of Sciences of the United States of America 95 (1998) 9448-9453.
[5] Lewellis SW, Knaut H, Attractive guidance: how the chemokine SDF1/CXCL12 guides different cells to different locations, Semin Cell Dev Biol 23 (2012) 333-340.
[6] Ma Q, Jones D, Springer TA, The chemokine receptor CXCR4 is required for the retention of B lineage and granulocytic precursors within the bone marrow microenvironment, Immunity 10 (1999) 463-471.
[7] Li M, Hale JS, Rich JN, Ransohoff RM, Lathia JD, Chemokine CXCL12 in neurodegenerative diseases: an SOS signal for stem cell-based repair, Trends Neurosci 35 (2012) 619-628.
[8] Bleul CC, Farzan M, Choe H, Parolin C, Clark-Lewis I, Sodroski J, Springer TA, The lymphocyte chemoattractant SDF-1 is a ligand for LESTR/fusin and blocks HIV-1 entry, Nature 382 (1996) 829-833.
[9] Graham GJ, Locati M, Mantovani A, Rot A, Thelen M, The biochemistry and biology of the atypical chemokine receptors, Immunology Letters 145 (2012) 30-38.
[10] Williams JL, Holman DW, Klein RS, Chemokines in the balance: maintenance of homeostasis and protection at CNS barriers, Frontiers in Cellular Neuroscience 8 (2014).
[11] Naumann U, Cameroni E, Pruenster M, Mahabaleshwar H, Raz E, Zerwes HG, Rot A, Thelen M, CXCR7 Functions as a Scavenger for CXCL12 and CXCL11, Plos One 5 (2010).
[12] Patel JR, McCandless EE, Dorsey D, Klein RS, CXCR4 promotes differentiation of oligodendrocyte progenitors and remyelination, Proc Natl Acad Sci U S A 107 (2010) 11062-11067.
[13] Odemis V, Boosmann K, Heinen A, Kury P, Engele J, CXCR7 is an active component of SDF-1 signalling in astrocytes and Schwann cells, J Cell Sci 123 (2010) 1081-1088.
[14] Pawig L, Klasen C, Weber C, Bernhagen J, Noels H, Diversity and inter-connections in the CXCR4 chemokine receptor/ligand family: molecular perspectives, Frontiers in Immunology 6 (2015).
[15] Williams JL, Patel JR, Daniels BP, Klein RS, Targeting CXCR7/ACKR3 as a therapeutic strategy to promote remyelination in the adult central nervous system, Journal of Experimental Medicine 211 (2014) 791-799.
[16] Cartier L, Hartley O, Dubois-Dauphin M, Krause KH, Chemokine receptors in the central nervous system: role in brain inflammation and neurodegenerative diseases, Brain Res Brain Res Rev 48 (2005) 16-42.
[17] Li M, Ransohoff RM, Multiple roles of chemokine CXCL12 in the central nervous system: a migration from immunology to neurobiology, Prog Neurobiol 84 (2008) 116-131.
[18] Mithal DS, Banisadr G, Miller RJ, CXCL12 signaling in the development of the nervous system, J Neuroimmune Pharmacol 7 (2012) 820-834.
[19] Bakondi E, Catalgol B, Bak I, Jung T, Bozaykut P, Bayramicli M, Ozer NK, Grune T, Age-related loss of stress-induced nuclear proteasome activation is due to low PARP-1 activity, Free Radical Biology and Medicine 50 (2011) 86-92.

[20] Carbajal KS, Miranda JL, Tsukamoto MR, Lane TE, CXCR4 Signaling Regulates Remyelination by Endogenous Oligodendrocyte Progenitor Cells in a Viral Model of Demyelination, Glia 59 (2011) 1813-1821.
[21] Li Y, Tang G, Liu Y, He X, Huang J, Lin X, Zhang Z, Yang G-Y, Wang Y, CXCL12 Gene Therapy Ameliorates Ischemia-Induced White Matter Injury in Mouse Brain, Stem cells translational medicine 4 (2015).
[22] Thelen M, Thelen S, CXCR7, CXCR4 and CXCL12: an eccentric trio?, J Neuroimmunol 198 (2008) 9-13.
[23] Lecca D, Ceruti S, Uracil nucleotides: from metabolic intermediates to neuroprotection and neuroinflammation, Biochem Pharmacol 75 (2008) 1869-1881.
[24] Fumagalli M, Daniele S, Lecca D, Lee PR, Parravicini C, Fields RD, Rosa P, Antonucci F, Verderio C, Trincavelli ML, Bramanti P, Martini C, Abbracchio MP, Phenotypic changes, signaling pathway, and functional correlates of GPR17-expressing neural precursor cells during oligodendrocyte differentiation, J Biol Chem 286 (2011) 10593-10604.
[25] Ciana P, Fumagalli M, Trincavelli ML, Verderio C, Rosa P, Lecca D, Ferrario S, Parravicini C, Capra V, Gelosa P, Guerrini U, Belcredito S, Cimino M, Sironi L, Tremoli E, Rovati GE, Martini C, Abbracchio MP, The orphan receptor GPR17 identified as a new dual uracil nucleotides/cysteinyl-leukotrienes receptor, Embo Journal 25 (2006) 4615-4627.
[26] Benned-Jensen T, Rosenkilde MM, Distinct expression and ligand-binding profiles of two constitutively active GPR17 splice variants, British Journal of Pharmacology 159 (2010) 1092-1105.
[27] Buccioni M, Marucci G, Dal Ben D, Giacobbe D, Lambertucci C, Soverchia L, Thomas A, Volpini R, Cristalli G, Innovative functional cAMP assay for studying G protein-coupled receptors: application to the pharmacological characterization of GPR17, Purinergic Signal 7 (2011) 463-468.
[28] Maekawa A, Balestrieri B, Austen KF, Kanaoka Y, GPR17 is a negative regulator of the cysteinyl leukotriene 1 receptor response to leukotriene D4, Proc Natl Acad Sci U S A 106 (2009) 11685-11690.
[29] Qi AD, Harden TK, Nicholas RA, Is GPR17 a P2Y/leukotriene receptor? examination of uracil nucleotides, nucleotide sugars, and cysteinyl leukotrienes as agonists of GPR17, The Journal of pharmacology and experimental therapeutics 347 (2013) 38-46.
[30] Krumbholz M, Theil D, Cepok S, Hemmer B, Kivisakk P, Ransohoff RM, Hofbauer M, Farina C, Derfuss T, Hartle C, Newcombe J, Hohlfeld R, Meinl E, Chemokines in multiple sclerosis: CXCL12 and CXCL13 up-regulation is differentially linked to CNS immune cell recruitment, Brain 129 (2006) 200-211.
[31] Moll NM, Cossoy MB, Fisher E, Staugaitis SM, Tucky BH, Rietsch AM, Chang A, Fox RJ, Trapp BD, Ransohoff RM, Imaging correlates of leukocyte accumulation and CXCR4/CXCL12 in multiple sclerosis, Arch Neurol 66 (2009) 44-53.
[32] Franciotta D, Zardini E, Ravaglia S, Piccolo G, Andreoni L, Bergamaschi R, Romani A, Tavazzi E, Naldi P, Ceroni M, Marchioni E, Cytokines and chemokines in cerebrospinal fluid and serum of adult patients with acute disseminated encephalomyelitis, J Neurol Sci 247 (2006) 202-207.
[33] Fumagalli M, Bonfanti E, Daniele S, Zappelli E, Lecca D, Martini C, Trincavelli ML, Abbracchio MP, The ubiquitin ligase Mdm2 controls oligodendrocyte maturation by intertwining mTOR with G protein-coupled receptor kinase 2 in the regulation of GPR17 receptor desensitization, Glia 63 (2015).
[34] Fumagalli M, Lecca D, Abbracchio MP, CNS remyelination as a novel reparative approach to neurodegenerative diseases: The roles of purinergic signaling and the P2Y-like receptor GPR17, Neuropharmacology (2015).
[35] Raccosta L, Fontana R, Maggioni D, Lanterna C, Villablanca EJ, Paniccia A, Musumeci A, Chiricozzi E, Trincavelli ML, Daniele S, Martini C, Gustafsson JA, Doglioni C, Feo SG, Leiva A, Ciampa MG, Mauri L, Sensi C, Prinetti A, Eberini I, Mora JR, Bordignon C, Steffensen KR, Sonnino S, Sozzani S, Traversari C, Russo V, The oxysterol-CXCR2 axis plays a key role in the recruitment of tumor-promoting neutrophils, J Exp Med 210 (2013) 1711-1728.

[36] Sensi C, Daniele S, Parravicini C, Zappelli E, Russo V, Trincavelli ML, Martini C, Abbracchio MP, Eberini I, Oxysterols act as promiscuous ligands of class-A GPCRs: In silico molecular modeling and in vitro validation, Cell Signal (2014).
[37] Fredriksson R, Lagerstrom MC, Lundin LG, Schioth HB, The G-protein-coupled receptors in the human genome form five main families. Phylogenetic analysis, paralogon groups, and fingerprints, Mol Pharmacol 63 (2003) 1256-1272.
[38] Raport CJ, Schweickart VL, Chantry D, Eddy RL, Shows TB, Godiska R, Gray PW, New members of the chemokine receptor gene family, Journal of Leukocyte Biology 59 (1996) 18-23.
[39] Tamamis P, Floudas CA, Elucidating a key component of cancer metastasis: CXCL12 (SDF-1alpha) binding to CXCR4, J Chem Inf Model 54 (2014) 1174-1188.
[40] Eberini I, Daniele S, Parravicini C, Sensi C, Trincavelli ML, Martini C, Abbracchio MP, In silico identification of new ligands for GPR17: a promising therapeutic target for neurodegenerative diseases, J Comput Aided Mol Des 25 (2011) 743-752.
[41] Parravicini C, Ranghino G, Abbracchio MP, Fantucci P, GPR17: molecular modeling and dynamics studies of the 3-D structure and purinergic ligand binding features in comparison with P2Y receptors, BMC Bioinformatics 9 (2008) 263.
[42] Im W, Feig M, Brooks CL, An Implicit Membrane Generalized Born Theory for the Study of Structure, Stability, and Interactions of Membrane Proteins, Biophysical Journal 85 (2003) 2900-2918.
[43] MacKerell AD, Bashford D, Bellott M, Dunbrack RL, Evanseck JD, Field MJ, Fischer S, Gao J, Guo H, Ha S, Joseph-McCarthy D, Kuchnir L, Kuczera K, Lau FTK, Mattos C, Michnick S, Ngo T, Nguyen DT, Prodhom B, Reiher WE, Roux B, Schlenkrich M, Smith JC, Stote R, Straub J, Watanabe M, Wiorkiewicz-Kuczera J, Yin D, Karplus M, All-atom empirical potential for molecular modeling and dynamics studies of proteins, Journal of Physical Chemistry B 102 (1998) 3586-3616.
[44] Fanelli F, Felline A, Dimerization and ligand binding affect the structure network of A2A adenosine receptor, Biochimica et Biophysica Acta (BBA) - Biomembranes 1808 (2011) 1256-1266.
[45] Lomize MA, Pogozheva ID, Joo H, Mosberg HI, Lomize AL, OPM database and PPM web server: resources for positioning of proteins in membranes, Nucleic Acids Research 40 (2012) D370-D376.
[46] Berendsen HJC, Postma JPM, van Gunsteren WF, DiNola A, Haak JR, Molecular dynamics with coupling to an external bath, Journal of Chemical Physics 81 (1984) 3684-3690.
[47] Van der Spoel D, Lindahl E, Hess B, Groenhof G, Mark AE, Berendsen HJC, GROMACS: Fast, flexible, and free, Journal of Computational Chemistry 26 (2005) 1701-1718.
[48] Humphrey W, Dalke A, Schulten K, VMD: visual molecular dynamics, J Mol Graph 14 (1996) 33-38, 27-38.
[49] Shadnia H, Wright JS, Anderson JM, Interaction force diagrams: new insight into ligand-receptor binding, Journal of Computer-Aided Molecular Design 23 (2009) 185-194.
[50] Daniele S, Trincavelli ML, Gabelloni P, Lecca D, Rosa P, Abbracchio MP, Martini C, Agonist-induced desensitization/resensitization of human G protein-coupled receptor 17: a functional cross-talk between purinergic and cysteinyl-leukotriene ligands, The Journal of pharmacology and experimental therapeutics 338 (2011) 559-567.
[51] Calleri E, Ceruti S, Cristalli G, Martini C, Temporini C, Parravicini C, Volpini R, Daniele S, Caccialanza G, Lecca D, Lambertucci C, Trincavelli ML, Marucci G, Wainer IW, Ranghino G, Fantucci P, Abbracchio MP, Massolini G, Frontal Affinity Chromatography-Mass Spectrometry Useful for Characterization of New Ligands for GPR17 Receptor, Journal of Medicinal Chemistry 53 (2010) 3489-3501.
[52] Ciana P, Fumagalli M, Trincavelli ML, Verderio C, Rosa P, Lecca D, Ferrario S, Parravicini C, Capra V, Gelosa P, Guerrini U, Belcredito S, Cimino M, Sironi L, Tremoli E, Rovati GE, Martini C, Abbracchio MP, The orphan receptor GPR17 identified as a new dual uracil nucleotides/cysteinyl-leukotrienes receptor, Embo J 25 (2006) 4615-4627.

[53] Parravicini C, Abbracchio MP, Fantucci P, Ranghino G, Forced unbinding of GPR17 ligands from wild type and R255I mutant receptor models through a computational approach, BMC Struct Biol 10 (2010) 8.
[54] Zhang K, Zhang J, Gao ZG, Zhang D, Zhu L, Han GW, Moss SM, Paoletta S, Kiselev E, Lu W, Fenalti G, Zhang W, Muller CE, Yang H, Jiang H, Cherezov V, Katritch V, Jacobson KA, Stevens RC, Wu B, Zhao Q, Structure of the human P2Y12 receptor in complex with an antithrombotic drug, Nature 509 (2014) 115-118.
[55] de Graaf C, Foata N, Engkvist O, Rognan D, Molecular modeling of the second extracellular loop of G-protein coupled receptors and its implication on structure-based virtual screening, Proteins-Structure Function and Bioinformatics 71 (2008) 599-620.
[56] Peeters MC, van Westen GJP, Li Q, Ijzerman AP, Importance of the extracellular loops in G protein-coupled receptors for ligand recognition and receptor activation, Trends in Pharmacological Sciences 32 (2011) 35-42.
[57] Zhao Q, Wu BL, Ice breaking in GPCR structural biology, Acta Pharmacologica Sinica 33 (2012) 324-334.
[58] Veldkamp CT, Seibert C, Peterson FC, De la Cruz NB, Haugner JC, Basnet H, Sakmar TP, Volkman BF, Structural Basis of CXCR4 Sulfotyrosine Recognition by the Chemokine SDF-1/CXCL12, Science Signaling 1 (2008).
[59] Huang XQ, Shen JH, Cui M, Shen LL, Luo XM, Ling K, Pei G, Jiang HL, Chen KX, Molecular dynamics simulations on SDF-1 alpha: Binding with CXCR4 receptor, Biophysical Journal 84 (2003) 171-184.
[60] Xu L, Li YY, Sun HY, Li D, Hou TJ, Structural basis of the interactions between CXCR4 and CXCL12/SDF-1 revealed by theoretical approaches, Molecular Biosystems 9 (2013) 2107-2117.
[61] Crump MP, Gong JH, Loetscher P, Rajarathnam K, Amara A, Arenzana-Seisdedos F, Virelizier JL, Baggiolini M, Sykes BD, Clark-Lewis I, Solution structure and basis for functional activity of stromal cell-derived factor-1; dissociation of CXCR4 activation from binding and inhibition of HIV-1, Embo Journal 16 (1997) 6996-7007.
[62] Rajagopalan L, Rajarathnam K, Structural basis of chemokine receptor function - A model for binding affinity and ligand selectivity, Bioscience Reports 26 (2006) 325-339.
[63] Wolf S, Grunewald S, Sequence, structure and ligand binding evolution of rhodopsin-like G protein-coupled receptors: a crystal structure-based phylogenetic analysis, PLoS One 10 (2015) e0123533.
[64] Daniele S, Trincavelli ML, Fumagalli M, Zappelli E, Lecca D, Bonfanti E, Campiglia P, Abbracchio MP, Martini C, Does GRK-beta arrestin machinery work as a "switch on" for GPR17-mediated activation of intracellular signaling pathways?, Cell Signal 26 (2014) 1310-1325.
[65] Maysami S, Nguyen D, Zobel F, Pitz C, Heine S, Hopfner M, Stangel M, Modulation of rat oligodendrocyte precursor cells by the chemokine CXCL12, Neuroreport 17 (2006) 1187-1190.
[66] Kothur K, Wienholt L, Brilot F, Dale RC, CSF cytokines/chemokines as biomarkers in neuroinflammatory CNS disorders: A systematic review, Cytokine (2015).
[67] Pashenkov M, Soderstrom M, Link H, Secondary lymphoid organ chemokines are elevated in the cerebrospinal fluid during central nervous system inflammation, J Neuroimmunol 135 (2003) 154-160.

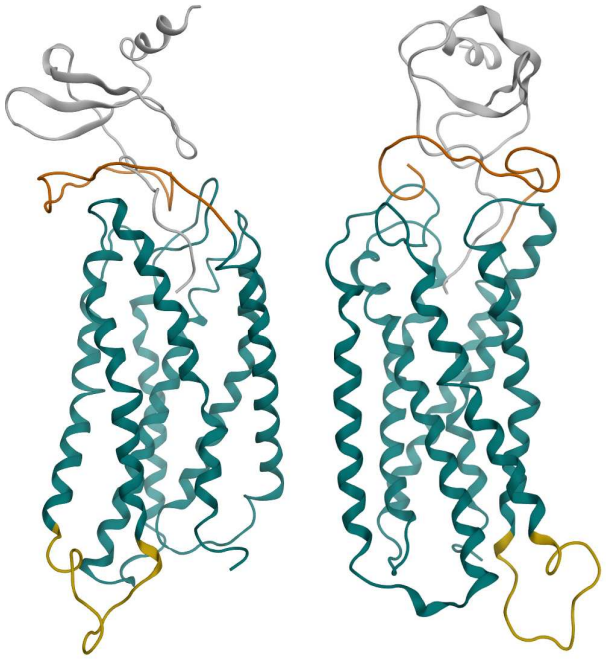

Figure 1

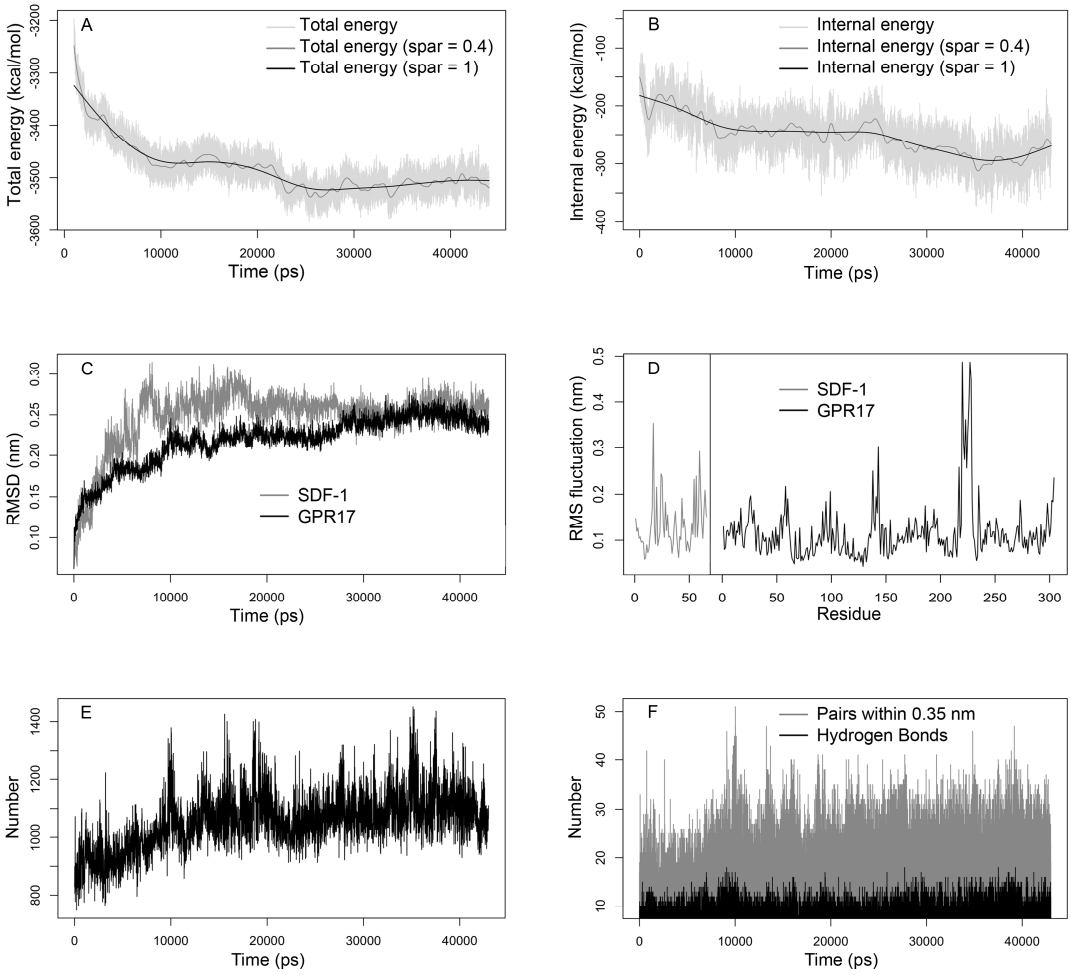

Figure 2

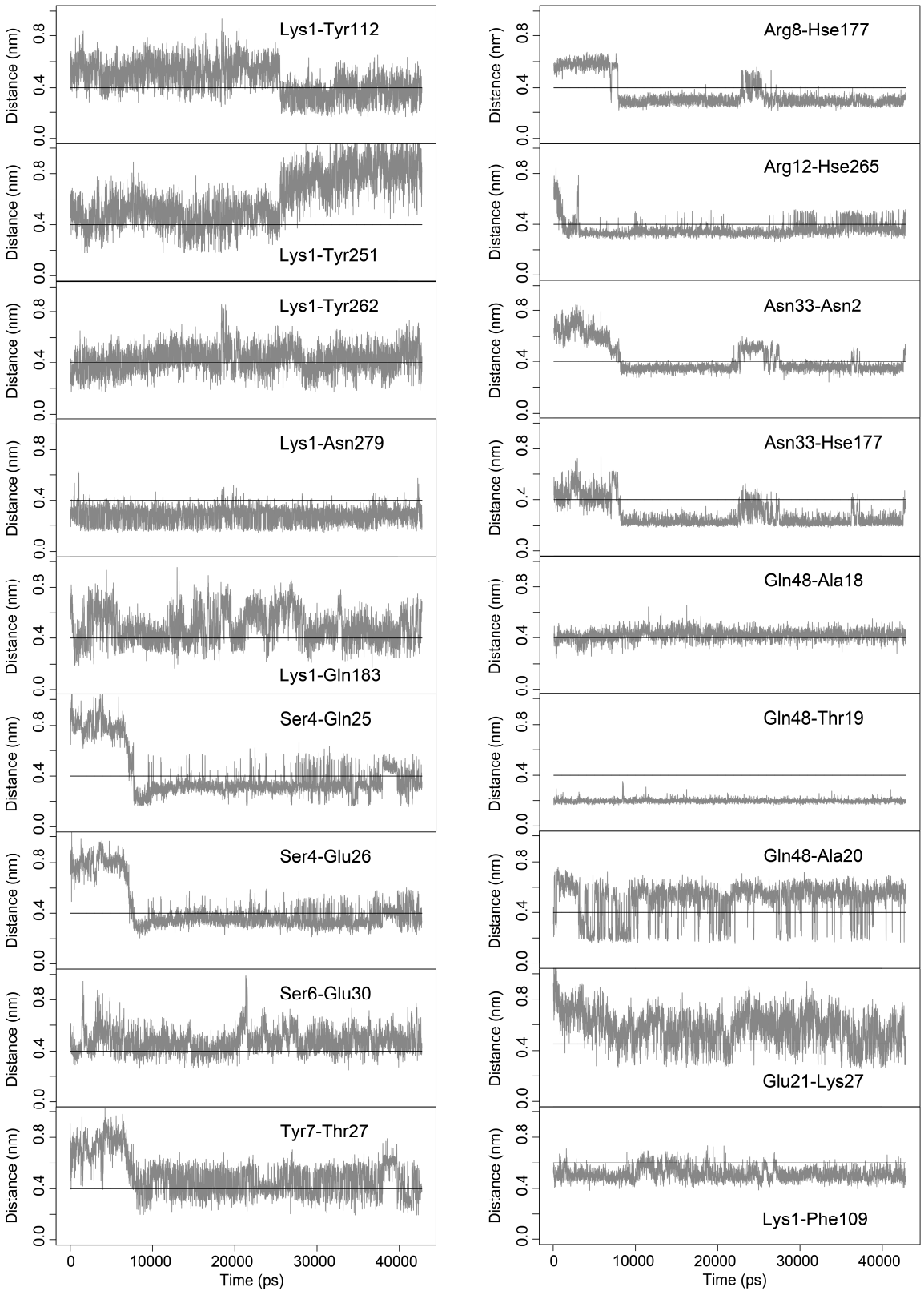

Figure 3

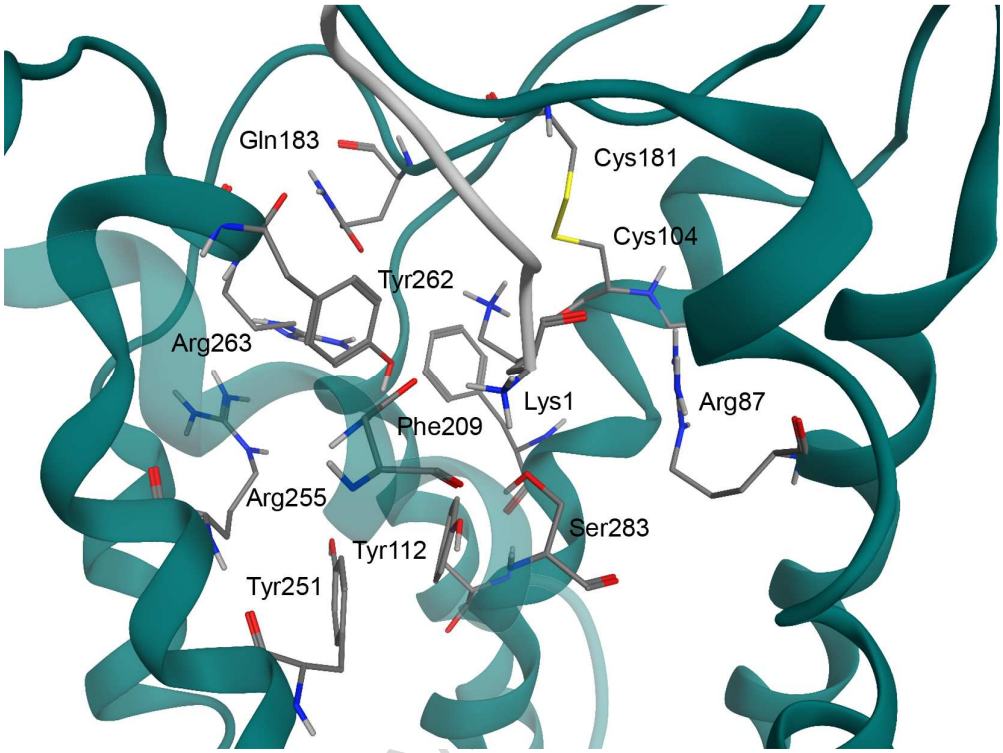

Figure 4

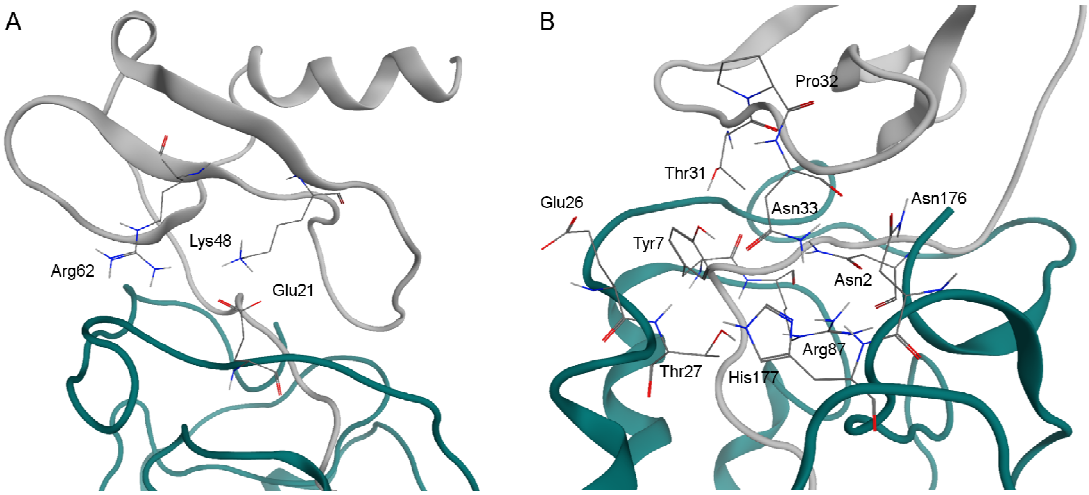

Figure 5

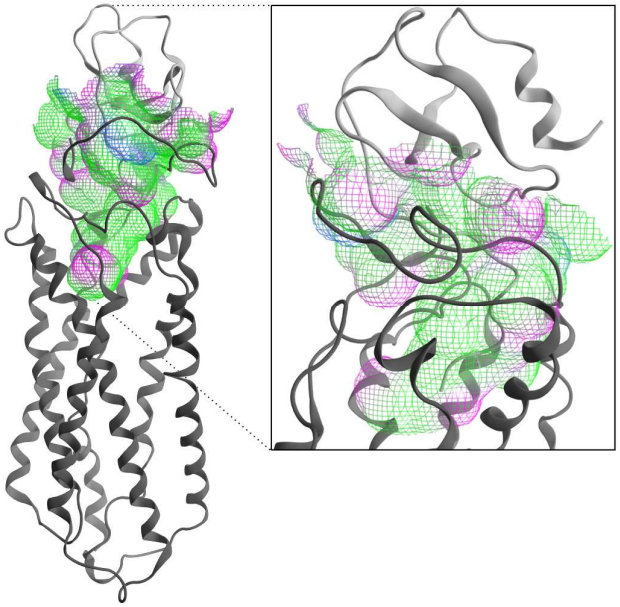

Figure 6

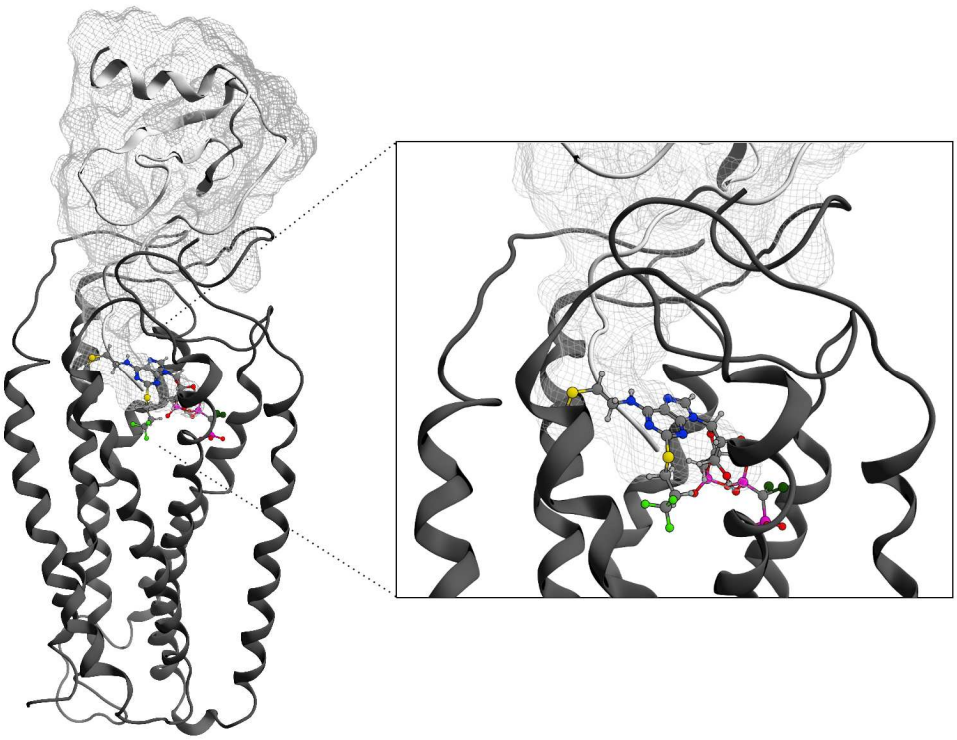

Figure 7

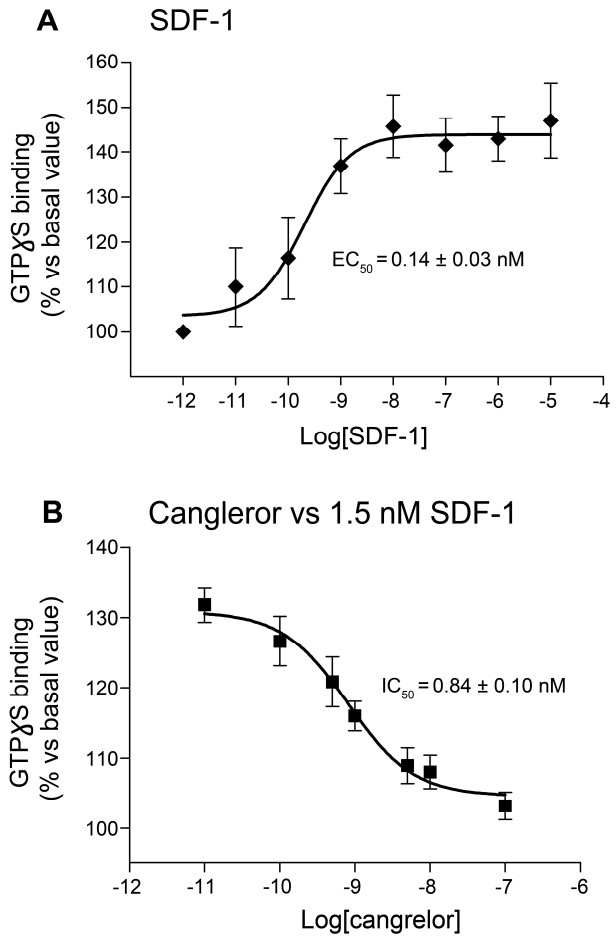

Figure 8

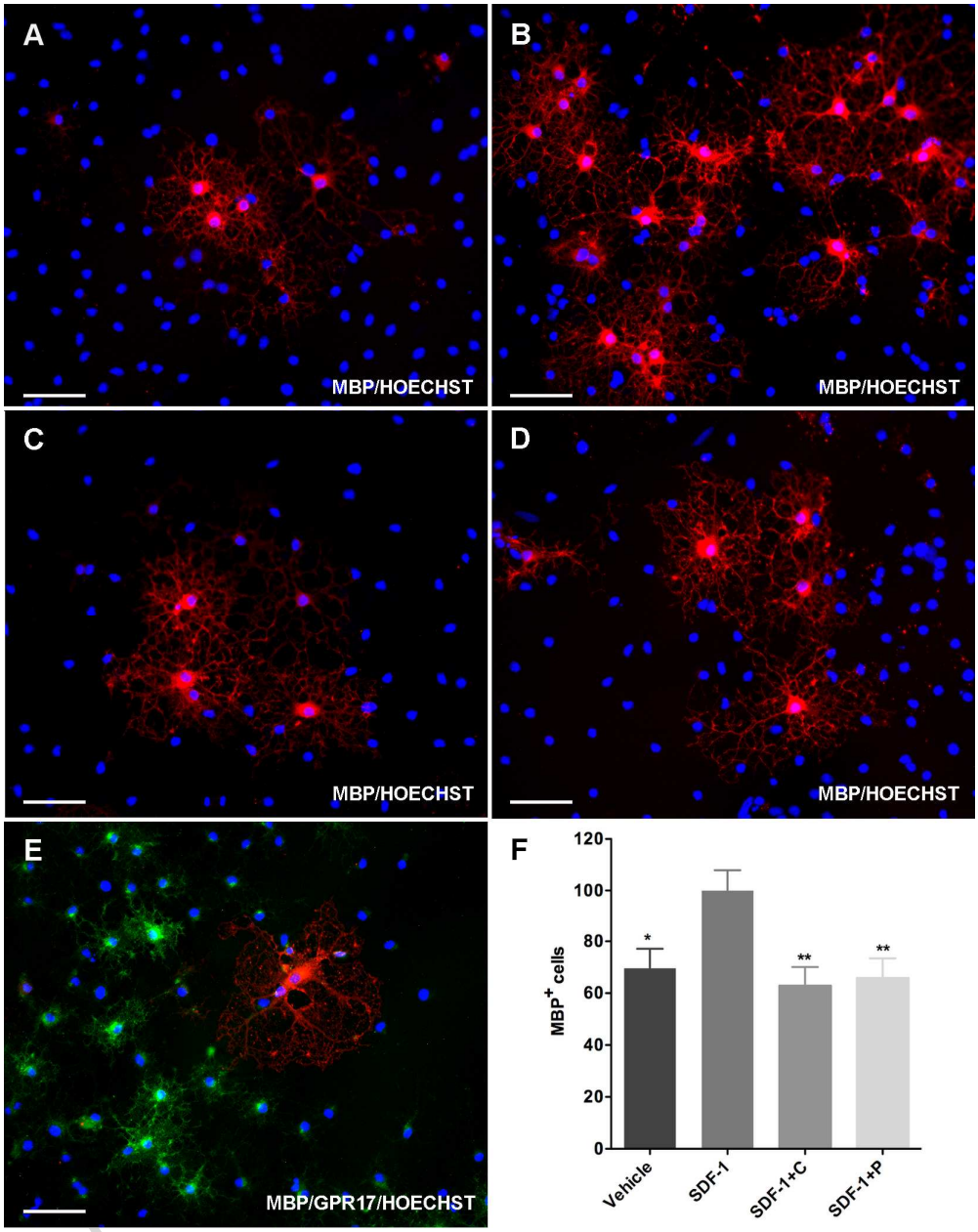

Figure 9

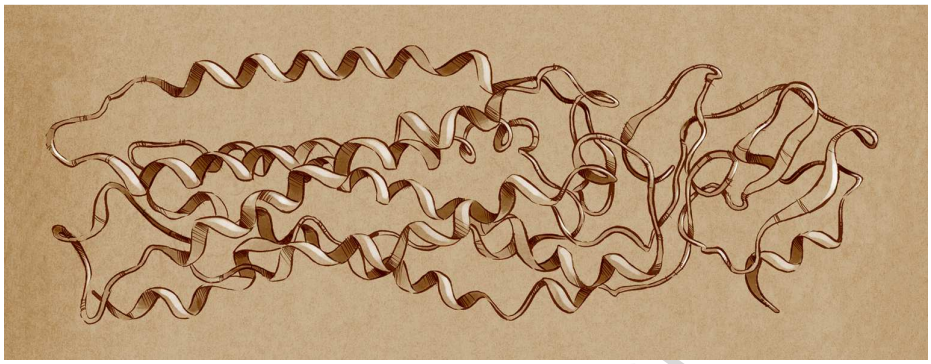

Graphical Abstract